
ELSEVIER

Nuclear Instruments and Methods in Physics Research B 166–167 (2000) 771–781

NIM B
Beam Interactions with Materials & Atoms

www.elsevier.nl/locate/nimb

Photosensitive point defects in optical glasses: Science and applications

B.G. Potter Jr. *, K. Simmons-Potter

Sandia National Laboratories, Albuquerque, NM 87185, USA

Abstract

The understanding and manipulation of the point defect structure in oxide glasses have been critical to the enhanced performance and reliability of optical-fiber-based, photosensitive photonic devices that currently find widespread application in telecommunications and remote sensing technologies. We provide a brief review of past research investigating photosensitive mechanisms in germanosilicate glasses, the primary material system used in telecommunications fibers. This discussion motivates an overview of ongoing work within our laboratories to migrate photosensitive glass technologies to a planar format for integrated photonic applications. Using reactive-atmosphere, RF-magnetron sputtering, we have demonstrated control of glass defect structure during synthesis, thereby controlling both the material photosensitivity (i.e., dispersion and magnitude of the refractive index change) and its environmental stability.

PACS: 42.70.Hj; 42.70.Ce
Keywords: Photosensitivity; Point defects; Glass; Optical phenomena; Photonics

1. Introduction

The discovery of photoinduced, refractive index grating formation within the Ge-doped core of a silica optical fiber by Hill et al. [1] in 1978 began an intense period of research activity in the area of photosensitive defects in oxide glass. These research efforts have culminated in both a deeper understanding of the underlying mechanisms responsible for photosensitive (PS) effects and in the development of a wide array of in-fiber photonic devices for telecommunications and remote sensing.

While photosensitivity can be, in a general sense, associated with any optical modification of material electronic and/or atomic structure, resulting in changes in optical, electronic or chemical behavior, the primary photosensitive effect of interest here is a stable, photoinduced change in material refractive index. Given a photosensitive material, appropriate control of optical exposure conditions can be used to form a wide range of photonic devices (based on refractive index patterning) using only a single-step, direct-write optical processing technique. This approach thus has

* Corresponding author. Tel.: +1-505-844-9919; fax: +1-505-844-2974.
E-mail address: bgpotte@sandia.gov (B.G. Potter Jr.).

0168-583X/00/$ - see front matter
PII: S0168-583X(99)00864-2

the potential to provide a rapid, agile, and relatively inexpensive method for the manufacture of integrated photonic structures when contrasted with photolithographic technologies that typically require multiple chemical processing steps. Moreover, the discovery of a photosensitive response in the primary optical fiber material used in the optical telecommunications industry, Ge-doped SiO_2, has provided an important opportunity for the integration of optical devices within an established fiber system. Indeed, the potential for applications within the telecommunications and specialty fiber industries has been the primary motivating force for research activities in germanosilicate-based photosensitivity since 1978.

The present paper will begin with a brief introduction to the area of germanosilicate photosensitivity and its origins. We will focus particular attention on the impact of materials physics on the PS material response. Specifically, the identification and manipulation of point defects within the glass structure will be shown to be critical to the enhancement of photosensitivity and ultimately, to the performance of photonic devices.

The importance of a fundamental understanding of the photosensitive mechanism will then be illustrated in the context of ongoing work within our laboratories to migrate photosensitive glass technologies to a planar format, providing high photo-induced refractive index changes and tailored environmental sensitivity (e.g., thermal, radiation) with minimal post-synthesis processing. The planar geometry offers the potential of photosensitive device integration with microphotonic systems, bringing both optical signal manipulation and local physical state sensing 'on-chip'. Investigation of the photosensitive effect in thin films also has an advantage over optical fiber studies in that material composition and processing issues may be more fully decoupled from one another, enabling a more straightforward investigation of intrinsic photosensitive mechanisms.

In this paper, we will discuss our efforts to identify the relevant photosensitive mechanism in our materials and to relate our knowledge of the intrinsic optical behavior of the glass to device performance. As an example, we will describe our efforts to predict the diffraction behavior of a photosensitive Bragg grating under elevated temperature environments using known thermal annealing effects on optical absorption. The ability to model and predict the aging of grating performance is an issue of great importance as these materials are utilized in a wider range of applications.

2. Photosensitivity and PS technology in germanosilicate glasses

Photosensitivity can be characterized as a stable, refractive index perturbation produced by exposure of a material to optical radiation. In the case of germanosilicate glasses, index changes of up to 10^{-3} can be efficiently fabricated within a germanosilicate glass through exposure to ultraviolet light, typically in the 190–340 nm wavelength range [2–4]. Although PS effects in germanosilicates were first observed in 1978 [1], the technological promise of photosensitivity in glass optical fibers was not fully realized until both the fundamental origins of the effect were more fully elucidated and tractable optical patterning approaches were developed. In particular, the development of transverse exposure techniques (side-writing) [5,6] exploited the correlation between defect absorption bands in the material and its photosensitivity, enabling the rapid production of PS Bragg grating devices with tunable spectral response. This development dramatically increased the technological impact of these devices within the telecommunications and remote sensing fields.

2.1. Mechanisms

While the precise mechanism causing the photosensitive effect varies with material composition, processing history and writing conditions, the phenomenon has been generally linked to optical absorption associated with point defect centers present within the glass structure. Clearly the observation of photosensitivity requires coupling of the optical field to the material through allowed electronic states. The sub-band gap photosensitivity typically exhibited by germanosilicates (with

band gaps in the 6–9 eV range) relies on the existence of structural point defects that furnish electronic states in the band gap of the glass. Photoinduced redistribution of carriers within these states is an initial step in the material photosensitive response. Depending upon the excitation conditions and relaxation pathways available, the photoexcitation of the material can result in a permanent redistribution of carriers within the density of states and even in topological changes in the short- and medium-range atomic structure itself. Both of these effects can cause refractive index variations in the material.

Knowledge of the defect states in the glass is, thus, necessary to understand photosensitivity. The disordered-network glass structure present in germanosilicates can sustain a wide variety of structural 'defects', including vacancies, dangling bonds and dopant/impurity atoms. Table 1 provides a partial listing of defect states hypothesized to participate in the photosensitive response observed in the germanosilicates. In general, at least two germanium oxygen deficient centers (GODC), the neutral oxygen monovacancy (NOMV) and the neutral oxygen divacancy (NODV), have been associated with absorption bands at 5.08 eV (244 nm) and 5.16 eV (240 nm), respectively [7]. UV excitation (5.0 eV, 248 nm) into the lower energy band is thought to be the initial step in the photosensitive effect at low intensities (<40 mJ/cm^2/pulse). Such an optical exposure results in the bleaching of the NOMV band and in the formation of Ge E′ centers with an associated induced absorption in the 190 nm range [7–9]. At higher UV intensities, an alternative mechanism involving two-photon absorption from valence band states (linked to lone-pair electrons on bridging oxygens) to the conduction band is believed to result in the formation of germanium electron centers (GEC, also called Ge(1) and Ge(2) centers [10,11]) and a self-trapped hole center (STH) [8–10]. Under further illumination at 5.0 eV, there is evidence that the GECs are converted to Ge E′ centers and nonbridging oxygens [8]. Disagreement within the literature still exists, however, regarding the identity and role of precursor defects in the photosensitive process. For example, the intrinsic absorption band around 5.16 eV has been identified by Tsai et al. [12] as a germanium lone pair center (GLPC). Other work suggests that the GLPC is, in fact, the fundamental precursor state leading to the formation of both Ge E′ and GECs via a two-photon process involving the NOMV as an intermediate defect structure [13]. Moreover, the evolution of Ge E′ centers from GECs with continued 5.0 eV illumination was not observed in this latter study [13].

Thus, despite the large knowledge base available, identification of the primary photosensitive defects in glass is a difficult challenge. The high sensitivity of the glass structure to both composition and processing history requires close control of sample fabrication conditions; even glasses with nominally the same composition can exhibit dramatically different photo-induced responses. This effect makes the opportunity for detailed comparisons between different studies in different research groups rare. The situation is compounded, in fiber-based studies, by the unavoidable coupling of materials process parameters and material composition, dictated by the synthesis process itself. This convolution of experimental issues

Table 1
Partial listing of point defect states participating in germanosilicate glass photosensitive response (see literature references in text)

Absorption energy (eV)		Designation
5.08	Germanium Oxygen Deficient	Neutral Oxygen Monovacancy (NOMV)
5.16	Centers (GODC)	Neutral Oxygen Divacancy (NODV) or Germanium Lone Pair Center (GLPC)
4.6	Germanium Electron Centers	Ge(1)
5.8	(GEC)	Ge(2)
6.4		Ge E′

complicates a controlled materials study of photosensitivity.

As indicated in the previous paragraph, photosensitive studies in optical fibers and thin films have utilized a wide range of optical exposure conditions (e.g., UV pulse energies ranging from tens of mJ/cm^2/pulse to >1 J/cm^2/pulse; 190 nm to visible wavelengths). In addition, other work has investigated photosensitive effects indirectly by monitoring the behavior of photosensitive Bragg gratings rather than the underlying material properties responsible for the gratings themselves [14]. Such experimental diversity further occludes a unified description of intrinsic material behavior. In general, however, it is agreed that the UV-photosensitive response in germanosilicate glasses is linked to the presence of oxygen-deficient point defect centers associated with germanium in the glass structure. Moreover, the optical absorption bands associated with these structures have been used to explain the wavelength dependence of the photosensitive response [15].

Several mechanisms have been proposed to relate the photo-induced modification of defect structure to the change in refractive index observed in germanosilicates. The color center model proposes that photoinduced refractive index variation is the result of changes in optical absorption that accompany the photo-induced charge transfer and trapping between defect complexes in the glass. It is important to note that modification of the optical absorption spectrum over a narrow spectral range will perturb the refractive index over the entire ultraviolet to near infrared spectrum, as dictated by the Kramers–Kronig relations. The defect model which assigns the primary absorption center to an oxygen-deficient Ge-(Ge,Si) bond (NOMV), for example, has been used to successfully explain refractive index changes in some cases [15–18].

In addition to the color center model, processes involving more dramatic optical modification of the glass structure have also been proposed. While the initial optical absorption is still believed to be associated with oxygen-deficient structural defects in the material, these models also include local heating and higher order absorption processes. Such processes can result in modifications of the inherent stress state of the material [19] and even its density (compaction or volume expansion) [20,21]. The density modification, for instance, is then the primary contributor to a refractive index change. These mechanisms are typically observed in materials exposed under high incident UV pulse energies (>50 mJ/(cm^2-pulse)) and/or high energy photons (e.g., $\lambda = 193$ nm). Such writing conditions are employed in an effort to increase the refractive index change produced.

It appears likely that all of the mechanisms proposed could contribute to the refractive index changes observed. The relative contributions, however, will depend on both the materials and the exposure conditions used.

Based on the established link between photosensitivity and the presence of sub-band gap states associated with oxygen deficient Ge defect centers, several approaches have been used to enhance the photosensitive response of these glasses through either direct material modification or optical exposure conditions, with varied success. Such approaches include the use of hydrogen treatments at elevated temperatures [18,22] and pressures [23,24] which increase the density of photoactive defects in the material, the addition of dopants to provide additional optically active sub-band-gap states [25–27], ion implantation [28,29] and the manipulation of optical exposure conditions. The latter case includes variations in wavelength and intensity (to access single and multiphoton absorption regimes) [30] and the use of applied electric and strain fields during illumination [31,32].

3. Photosensitivity in thin-film waveguides

Photosensitive planar waveguides have been formed using a variety of synthetic approaches including PECVD [33,34], sol–gel [35–37], flame hydrolysis [38] and sputtering [39–41]. These efforts have resulted in photosensitive effects arising from phenomena including absorption band bleaching/growth and mechanically based mechanisms associated with structural relaxation driven by local stress/strain fields that lead to changes in volume and polarizability.

While these works illustrate the rich range of photo-mediated effects accessible through material processing, the present work will focus on our pioneering efforts in the use of reactive-atmosphere, RF-magnetron sputtering for the formation of germanosilicate thin films. This technique allows the in-situ control of oxygen-deficient defect structure, and hence, UV-photosensitivity through appropriate deposition parameter controls. Our efforts to understand the operative photosensitive mechanisms in these materials and to develop and evaluate basic photosensitive device structures will be reviewed. Optical and EPR spectroscopic analyses of thermal annealing effects will be discussed and used as a means to predict the stability of a Bragg grating in elevated temperature environments.

3.1. Reactive-atmosphere, RF-magnetron sputtered thin films

Given the established link between germanosilicate photosensitivity and the presence of oxygen-deficient germanium defects, a reactive-atmosphere, RF-magnetron sputtering approach was adopted. In this case, films were deposited from Si/Ge alloy targets under a partial oxygen atmosphere. Control of the oxygen partial pressure and substrate temperature during deposition was successful in controlling both the character and population of oxygen-deficient defects [41–43].

Fig. 1 contains UV absorption spectra for 2 μm thick, $50GeO_x$–$50SiO_y$ films deposited onto fused silica substrates at 180°C. With decreasing oxygen flow rate, i.e., decreasing film oxygen content, the absorption edge shifts to lower energies, exhibiting broad-band absorption in the ultraviolet. Thus it is apparent that through variation of oxygen partial pressure, the population of defect states may be carefully controlled.

Fig. 2 shows absorption spectra for 180°C (LT) and 600°C (HT) substrate temperature materials both in the as-deposited state and after a saturating exposure to a KrF excimer laser at 248 nm (20 mJ/cm^2/pulse, 15 Hz, 20 ns pulse length, total fluence = 10 kJ/cm^2). Inspection of the as-deposited spectra for the two types of materials indicate a clear difference in the absorption behavior with the higher substrate temperature material exhibiting discernable absorption bands at approximately 240 and 200 nm.

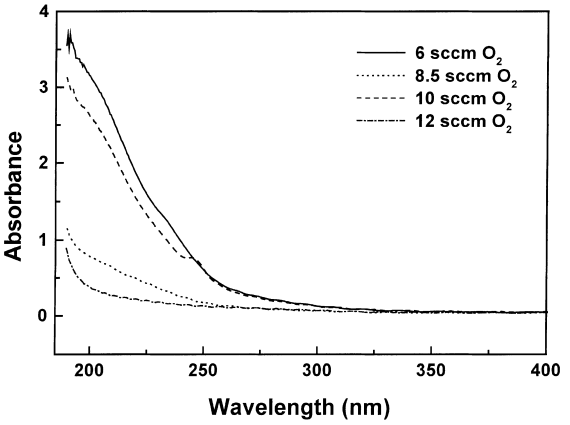

Fig. 1. Optical absorption spectra for $50GeO_x$–$50SiO_y$ films sputtered in a partial oxygen atmosphere. Decreasing oxygen flow rate (and, hence, partial pressure) during deposition leads to marked increase in UV optical absorption in the films.

In the low substrate temperature material (Fig. 2(a)), UV exposure results in broad-band absorption bleaching over the entire UV range while the high substrate temperature sample (Fig. 2(b)) bleaches in the 240 nm range and exhibits an induced absorption around 200 nm. The insets to Figs. 2(a) and (b) show the results of a Kramers–Kronig analysis of these photo-induced absorption changes. The calculations indicate that, through changes in the deposition conditions used, the defect structure and UV-response can be engineered to tune both the magnitude and sign of the induced refractive index change in the visible and near infrared. Direct measurement of the film optical constants using a prism coupling approach has confirmed the order of magnitude and sign (negative in the low-temperature depositions and positive in the high-temperature depositions) of the refractive index changes in these materials [44]. Such data lends strong support to a color center model for the photosensitivity observed in our films. In addition, subsequent AFM and profilometry studies have failed to indicate any variation in material volume or topography. Thus, the primary mechanism responsible for the low substrate temperature materials exhibiting the highest

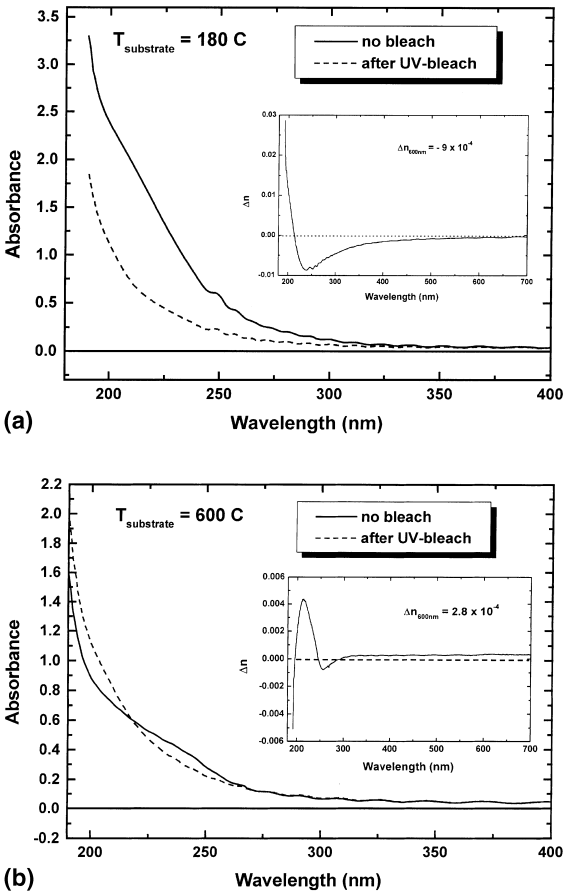

Fig. 2. (a) Optical absorption of films deposited to 180°C substrates following UV-laser exposure. Overall bleach of UV bands is seen to induce a negative refractive index change as calculated from Kramers–Kronig theory. (b) Optical absorption of films deposited to 600°C substrates following UV-laser exposure. Bleach of band at ~240 nm and growth of band at ~200 nm is observed to induce a positive refractive index change as calculated from Kramers–Kronig theory.

UV-induced Δn in an as-deposited germanosilicate, i.e., -4×10^{-3} (visible), may be attributed to color center dynamics in our films. In particular, the magnitude of the Δn is enhanced by a UV-bleaching response in which absorption strength over the entire UV range is reduced upon laser irradiation. This occurs without competition from band growth elsewhere in the optical spectrum.

The nature of defects participating in the photosensitive response was elucidated using optical absorption and EPR spectroscopies after both 5.0 eV irradiation and charge injection [42]. In contrast to more commonly observed photosensitive characteristics in germanosilicates, the low substrate temperature material actually exhibited a decreasing EPR center density with UV-irradiation at *g*-values consistent with those assigned to the Ge E′ center. However, charge injection studies indicated that charge trapping within the glass was not consistent with the presence of a traditional Ge E′ center [43]. The study culminated in the identification of precursor defect state that was EPR active and which, through photo-induced charge transfer, became diamagnetic. This hypothesized 'isolated' Ge dangling bond state was found to play an important role in the PS dynamics of the low-temperature, as-deposited films [43]. Fig. 3 contains a summary of photosensitive defect reactions in the sputtered materials. It is important to realize that, while the isolated Ge dangling bond state is certainly participating in the photosensitive response, the breadth of the UV absorption bleach in this material most likely indicates the presence of additional, diamagnetic defect structures that do not appear in an EPR analysis.

In contrast, the high substrate temperature material exhibited UV-irradiation and charge injection characteristics consistent with the conversion of an oxygen-deficient Ge defect state at 242 nm to a traditional Ge E′ center with an associated increase in absorption at 200 nm and an increase in paramagnetic center density. Thus, through defect-level engineering of this glass during synthesis, we have controlled both the magnitude and dispersion of the photosensitive refractive index change. As will be discussed later, this capability also results in a tunable thermal stability that directly impacts the performance of PS devices in these glasses.

3.2. Photoimprinted Bragg gratings and embedded strip waveguides

Photosensitive Bragg gratings were fabricated in the sputter-deposited materials using a phase mask technique [6]. Bragg gratings are distributed feedback (DFB) gratings that consist of a periodically varying refractive index pattern written along the waveguide core. Such gratings can pro-

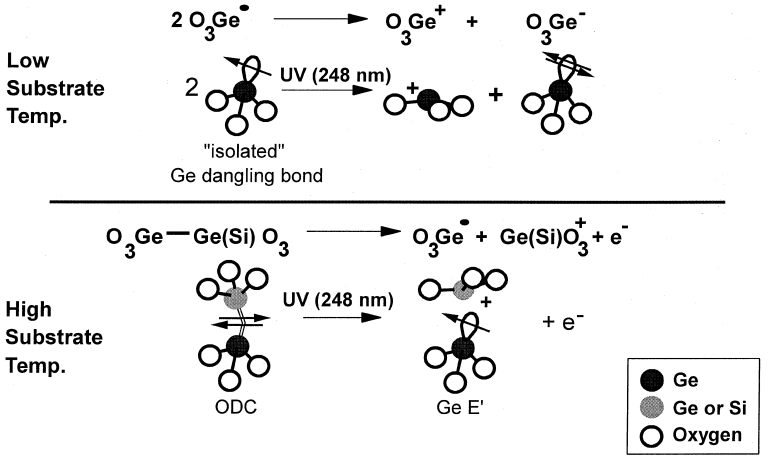

Fig. 3. Defect model for low (LT) and high (HT) temperature -depositions. The LT films are characterized by the presence of an isolated Ge dangling bond that is converted to the diamagnetic species by UV excitation. The HT films display the characteristic conversion of GODC defects to Ge E′ centers upon UV irradiation.

vide extremely high reflectivities (>90%) over very narrow bandwidths and they are widely used in optical fibers for signal manipulation and physical state sensing. (Several reviews of PS Bragg grating fabrication and applications are available [45–50]). Gratings were written using a KrF (248 nm) pulsed beam at 15 mJ/cm^2/pulse, 20 ns pulse length, and 15 Hz repetition rate until saturation of the UV absorption change. The enhanced photosensitivity provided by the low substrate temperature material allowed these gratings to be used both within the planar waveguide and in an out-of-plane mode enabling free-space diffraction of an incident beam [3]. Thus, in addition to the potential for high density integration of DFB-type devices into planar optical systems for signal manipulation and sensing, these highly photosensitive materials also provide a new optical functionality with an impact in microoptics for diffraction and imaging.

Using an aluminum negative shadow mask, multimode, embedded-strip waveguides were also produced [44]. The use of a negative mask structure was required given the negative photo-induced refractive index change exhibited by the low substrate temperature materials, thereby exposing the cladding regions of the strips to the UV illumination. (In the high substrate temperature films, a positive mask, allowing UV exposure of the waveguide core region, would be required given the positive refractive index change in that case.) Typical waveguide losses of 0.7 dB/cm in the visible and near IR were obtained in these structures.

3.3. Thermal stability

The study of the performance stability of both the material and the PS devices themselves is critical for assessing the utility of PS device structures in a variety of application environments. We have examined the thermal environment response both at the glass- and device-levels using isochronal anneal studies in a variety of oxidizing, reducing and neutral atmospheres both before and after UV-irradiation. A full synopsis of these results is beyond the scope of the present work and will be presented in subsequent publications. In general, optical absorption, EPR and Raman spectroscopic analyses indicate that there is significant structural relaxation in the low substrate temperature films in the 250°C–400°C anneal range. This results in a spectral redistribution of UV-absorption strength and is accompanied by a decrease in Ge-dangling-bond population as evidenced by EPR. Waveguide Raman data (Fig. 4) also support thermally mediated structural relaxation in the low substrate temperature materials, showing a reduction in non-bridging-oxygen vibrational band intensity (indicating increased

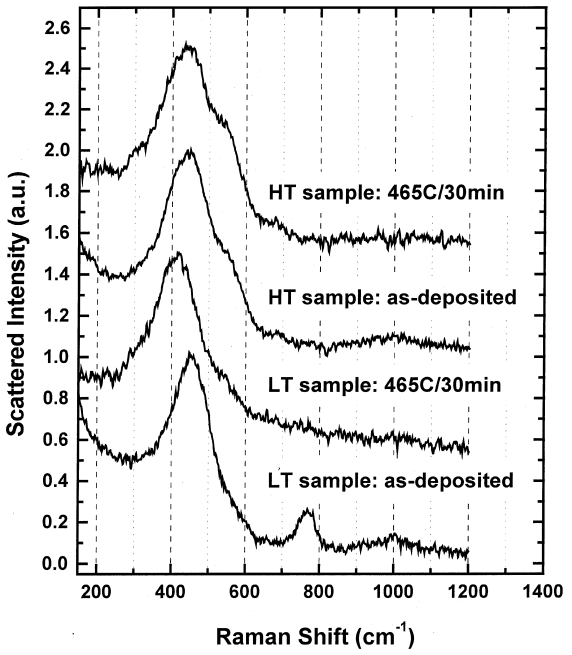

Fig. 4. Waveguide Raman spectra (unpolarized) collected from LT and HT samples subjected to thermal annealing at 465°C in flowing He. The HT material shows very little change in vibrational response after the anneal. In contrast, the LT sample exhibits a reduction in the 780 cm^{-1} band associated with non-bridging oxygen vibrations and a shift to lower energies (in the 430 cm^{-1} range) of the primary band associated with Ge–O–Ge, Ge–O–Si and Si–O–Si symmetric stretching vibrations. These results are consistent with increased connectivity in the glass network and a reduction in film stress with annealing in the LT material.

connectivity in the network) and bridging-oxygen symmetric stretching band shifts consistent with stress reduction in the thin film. This structural relaxation results in a final film structure most consistent with that of the high substrate temperature sputtered material or that of germanosilicates synthesized via other routes, including melting, vapor phase axial deposition and sol–gel.

These results are not surprising given the low substrate temperatures employed in the sputter deposition process. Such conditions inhibit the rearrangement of newly deposited atomic species into more energetically favorable configurations during film growth. Only after thermal energy is supplied during the annealing schedule, is the glass structure permitted to assume lower energy configurations consistent with higher temperature synthetic routes.

The UV-response of the low substrate temperature material is also transformed by the thermal anneal into that discussed above for the high substrate temperature films due to the change in defect structure. Fig. 5 contains representative absorption spectra and ESR spin densities from low substrate temperature thin films, summarizing the influence of annealing on both UV-bleached and as-deposited samples. Fig. 5 also includes spectra demonstrating the transformation of the photo-induced bleaching response in the low substrate temperature film after annealing.

On a device level, PS Bragg gratings written into both high and low substrate temperature films were annealed using the same isochronal schedule discussed above. The relative intensity of the 1st order diffracted beam (out-of-plane geometry) is presented in Fig. 6 as a function of anneal temperature for both types of films. Despite the established structural relaxation events evidenced by the low substrate temperature material in the

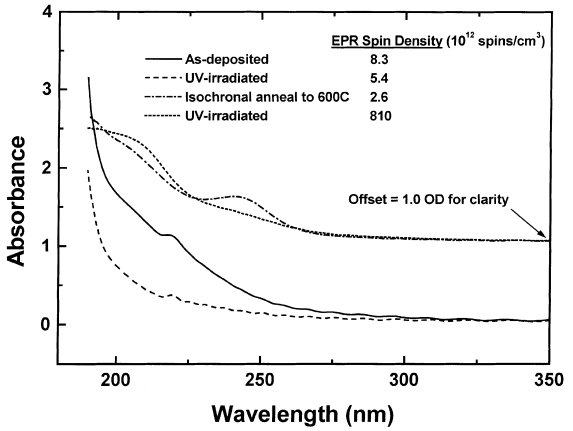

Fig. 5. Optical absorption spectra of LT-type films showing the effects of UV-exposure before and after isochronal annealing. As deposited, the LT films display an overall bleach of UV bands after excimer laser irradiation. Following anneal, samples now display bleach of only the 240 nm absorption with accompanying growth of 200 nm absorption. These data are indicative of a structural rearrangement following anneal. EPR spin densities associated with isolated, Ge dangling bond center (before annealing) and the Ge E′ center (after annealing) are given in the legend.

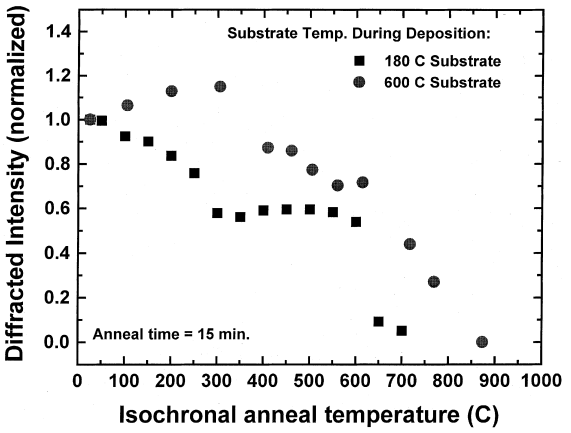

Fig. 6. The thermal stability of photo-induced Bragg gratings in both LT and HT-type films is illustrated through examination of out-of-plane, diffracted beam intensity as a function of isochronal anneal temperature.

studies discussed above, diffracted intensities >60% of the initial value are still maintained even up to 600°C. Indeed, both types of glasses show significant diffraction efficiency until $T > 600$°C.

Insight into the origins of the grating thermal behavior was obtained by modeling the response of a hypothetical grating in which the localized thermal response of low and high index regions were associated with the absorption behavior observed in UV-irradiated and as-deposited thin films in the intrinsic materials study. Kramers–Kronig analyses of the annealing-induced absorption changes provided an estimate of photo-induced grating contrast change that was, in turn, used to calculate diffraction efficiencies for this hypothetical grating. (The grating contrast is defined as the peak-to-peak index variation along grating length, and assuming a sinusoidal phase grating with an incident plane wave, the 1st order diffracted beam intensity is proportional to the square of the grating contrast.)

Figs. 7(a) and (b) show the modeled and experimental grating diffraction with isochronal annealing temperature for low and high substrate temperature films, respectively. In general, there is qualitative agreement between the calculated data and that obtained experimentally. The agreement is particularly good for the high substrate temperature material, even to the point of predicting

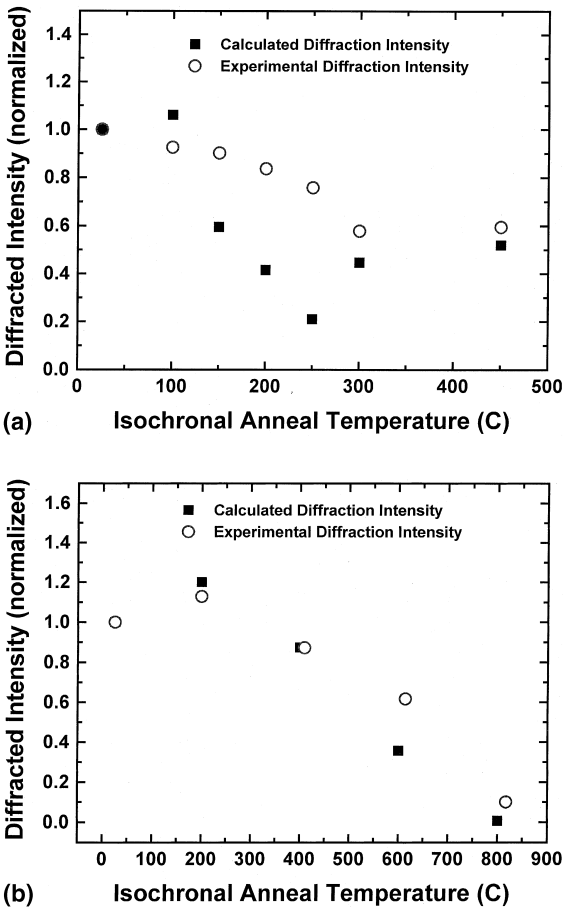

Fig. 7. Comparison of experimentally observed and modeled diffracted intensity for Bragg gratings in both the LT (a) and HT (b) materials. The calculated thermal response is obtained using a Kramers-Kronig analysis of thermally induced, material absorption change to determine the associated grating contrast change and diffraction efficiency variation of a hypothetical phase grating.

the enhancement in grating diffraction efficiency around 200°C. In contrast, the calculations for the low substrate temperature grating tend to underestimate the experimental results, especially in the 150–300°C range. However, the high diffraction efficiencies even at temperatures >400°C, are reproduced in the modeled response. The good agreement with experimental data exhibited lends support to our use of a color center model to describe the photosensitivity in these glasses since only a Kramers–Kronig contribution to refractive

index change is considered. The model deviations from the experimental behavior of the low substrate temperature film can be caused by several factors, including photo-induced density changes and absorption changes at higher energies not accounted for in the present calculation. Given the lack of evidence supporting volume changes in our materials, the latter factor is considered of primary interest. Vacuum-UV measurements are planned to further investigate the influence of higher energy absorption structure. Nonetheless, this initial study indicates that it is possible to qualitatively predict device-level performance based on a knowledge of intrinsic material optical behavior and operative photosensitive mechanism.

4. Conclusions

Photosensitivity in germanosilicate and related glass systems has evolved in the last two decades into a major technological area with a large, global market in the telecommunications industry. Bragg gratings that are photo-imprinted into the core of optical fibers provide an integrated solution to the need for low-loss, optical signal manipulation and remote physical state sensing. The technological impact of these devices was achieved only through the development of a fundamental understanding of the underlying photosensitive mechanisms operating in the glass itself. Based on the existence of intrinsic point defects and their interaction with the optical field, photosensitivity in these materials has been investigated by numerous research groups interested in materials synthesis, glass defect physics, device formation and device performance. These efforts have resulted in materials composition and processing approaches that can enhance the performance and reliability of PS fiber devices.

The migration of PS materials to a planar format offers the opportunity for the introduction of this technology into high areal density, integrated micro-photonic systems. In addition, thin film synthesis approaches can enable a more direct investigation of photosensitivity itself, free from the interdependence of fabrication and composition issues present in fiber-based studies. The inherent short path length nature of the planar geometry, however, places more stringent requirements on the photo-induced refractive index change furnished by the glass. The broader range of atomic structures accessed using the wide range of deposition techniques available, however, can be used to address this issue.

We have pioneered the use of reactive-atmosphere, RF-magnetron sputtering to synthesize highly photosensitive germanosilicate thin films without the need for post-deposition processing. Based on our ability to engineer the material defect structure during deposition, we have demonstrated tunable photosensitive response and environmental stability. This is understood in terms of the short and medium range structure present in the films, examined via optical, vibrational and magnetic spectroscopies. These efforts have resulted in the formation of photo-imprinted Bragg gratings and embedded-strip waveguides. Moreover, we have utilized our understanding of the intrinsic materials optical response under elevated temperature environments to predict device-level performance under these conditions. Through these activities, and those pursued in other research groups, high reliability, high performance planar PS devices will soon find numerous applications in integrated photonics.

Acknowledgements

The authors thank T. Dunbar for EPR analysis. Sandia National Laboratories is a multiprogram laboratory operated by Sandia Corporation, a Lockheed Martin Company. This work was supported by the U.S. DOE under contract DE-AC04-94AL85000.

References

[1] K.O. Hill, Y. Fujii, D.C. Johnson, B.S. Kawasaki, Appl. Phys. Lett. 32 (1978) 647.
[2] J. Albert, B. Malo, K.O. Hill, F. Bilodeau, D.C. Johnson, S. Theriault, Appl. Phys. Lett. 67 (1995) 3529.
[3] K. Simmons-Potter, B.G. Potter Jr., M. Sinclair, Jpn. J. Appl. Phys. Suppl. 37 (1) (1998) 8.

[4] D.S. Starodubov, V. Grubsky, J. Feinberg, B. Kobrin, S. Juma, Opt. Lett. 22 (1997) 1086.
[5] G. Meltz, W.W. Morey, W.H. Glenn, Opt. Lett. 14 (1989) 823.
[6] K.O. Hill, B. Malo, F. Bilodeau, D.C. Johnson, J. Albert, Appl. Phys. Lett. 62 (1993) 1035.
[7] H. Hosono, Y. Abe, D.L. Kinser, R.A. Weeks, K. Muta, K. Kawazoe, Phys. Rev. B 46 (11) (1992) 445.
[8] J. Nishii, K. Fukumi, H. Yamanaka, K. Kawamura, H. Hosono, H. Kawazoe, Phys. Rev. B 52 (1995) 1661.
[9] J. Nishii, N. Kitamura, H. Yamanaka, H. Hosono, H. Kawazoe, Opt. Lett. 20 (1995) 1184.
[10] H. Hosono, H. Kawazoe, J. Nishii, Phys. Rev. B 53 (R11) (1996) 921.
[11] E.J. Friebele, D.L. Griscom, Mat. Res. Soc. Symp. Proc. 61 (1986) 319.
[12] T.E. Tsai, E.J. Friebele, M. Rajaram, S. Mukhapadhyay, Appl. Phys. Lett. 64 (1994) 1481.
[13] M. Essid, J. Albert, J.L. Brebner, K. Awazu, J. Non-Cryst. Solids 246 (1999) 39.
[14] B. Poumellec, J. Non-Cryst. Solids 239 (1998) 108.
[15] K.D. Simmons, S. LaRochelle, V. Mizrahi, G.I. Stegeman, D.L. Griscom, Opt. Lett. 16 (1991) 141.
[16] D.P. Hand, P.St.J. Russell, Opt. Lett. 15 (1990) 102.
[17] R.M. Atkins, V. Mizrahi, T. Erdogan, Elec. Lett. 29 (1993) 385.
[18] K.D. Simmons, G.I. Stegeman, B.G. Potter Jr., J.H. Simmons, J. Non-Cryst. Solids 179 (1994) 254.
[19] D. Wong, S.B. Poole, M.G. Sceats, Opt. Lett. 17 (1992) 1773.
[20] J.P. Bernardin, N.M. Lawandy, Opt. Commun. 79 (1990) 194.
[21] P. Cordier, S. Dupont, M. Douay, G. Martinelli, P. Bernage, P. Niay, J.F. Bayon, L. Dong, Appl. Phys. Lett. 70 (1997) 1204.
[22] H. Hosono, H. Kawazoe, K. Muta, Appl. Phys. Lett. 63 (1993) 479.
[23] P.J. Lemaire, R.M. Atkins, V. Mizrahi, W.A. Reed, Elec. Lett. 29 (1993) 1191.
[24] R.M. Atkins, R.P. Espindola, Appl. Phys. Lett. 70 (1997) 1068.
[25] L. Reekie, L. Dong, SPIE 2998 (1997) 2; and references therein.
[26] M.M. Broer, R.L. Cone, J.R. Simpson, Opt. Lett. 16 (1991) 1391.
[27] F.M. Durville, E.G. Behrens, R.C. Powell, Phys. Rev. B 34 (1986) 4213.
[28] H. Hosono, K. Kawamura, N. Ueda, H. Kawazoe, S. Fujitsu, N. Matsunami, J. Phys. Condens. Matter 7 (1995) L343.
[29] M. Verhaegen, J.L. Brebner, L.B. Allard, J. Albert, Appl. Phys. Lett. 68 (1996) 3084.
[30] L.B. Allard, J. Albert, J.L. Brebner, G.R. Atkins, Opt. Lett. 22 (1997) 819.
[31] Y. Quiquempois, G. Martinelli, P. Niay, P. Bernage, M. Douay, J.F. Bayon, H. Poignant, Opt. Lett. 24 (1999) 139.
[32] Q. Zhang, D.A. Brown, L. Reinhart, T.F. Morse, J.Q. Wang, G. Xiao, IEEE Photon. Technol. Lett. 6 (1994) 839.
[33] J. Hubner, J.-M. Jouanno, J.E. Pedersen, R. Kromann, T. Feuchter, M. Kristensen, SPIE 2998 (1997) 100.
[34] J. Canning, D.J. Moss, M. Faith, P. Leach, P. Kemeny, C.V. Poulsen, O. Leistiko, Elec. Lett. 32 (1996) 1479.
[35] B.G. Potter Jr., R. Ochoa, D.G. Chen, J.H. Simmons, Opt. Lett. 17 (1992) 1349.
[36] K.D. Simmons, G.I. Stegeman, B.G. Potter Jr., J.H. Simmons, Opt. Lett. 18 (1993) 25.
[37] H. Shigemura, Y. Kawamoto, J. Nishii, M. Takahashi, J. Appl. Phys. 85 (1999) 3413.
[38] T. Erdogan, A. Partovi, V. Mizrahi, P.J. Lemaire, W.L. Wilson, T.A. Strasser, A.M. Glass, Appl. Optics 34 (1995) 6738.
[39] J. Nishii, H. Yamanaka, H. Hosono, H. Kawazoe, Opt. Lett. 21 (1996) 1360.
[40] K. Simmons-Potter, B.G. Potter Jr., D.C. McIntyre, P.D. Grandon, Appl. Phys. Lett. 68 (1996) 2011.
[41] B.G. Potter Jr., K. Simmons-Potter, W.L. Warren, J.A. Ruffner, D.C. Meister, SPIE 2998 (1997) 146.
[42] K. Simmons-Potter, B.G. Potter Jr., W.L. Warren, SPIE 2998 (1997) 93.
[43] W.L. Warren, K. Simmons-Potter, B.G. Potter Jr., J.A. Ruffner, Appl. Phys. Lett. 69 (1996) 1453.
[44] K. Simmons-Potter, B.G. Potter Jr., D.C. Meister, M.B. Sinclair, J. Non-Cryst. Solids 239 (1998) 96.
[45] A. Inoue, M. Shigehara, M. Ito, M. Inai, Y. Hattori, T. Mizunami, Optoelec. -Dev. Technol. 10 (1995) 119.
[46] R.J. Campbell, R. Kashyap, Int. J. Optoelec. 9 (1994) 33.
[47] K.O. Hill, G. Meltz, J. Lightwave Technol. 15 (1997) 1263.
[48] I. Bennion, J.A.R. Williams, L. Zhange, K. Sugden, N.J. Doran, Opt. Quant. Elec. 28 (1996) 93.
[49] A.D. Kersey, M.A. Davis, H.J. Patrick, M. Leblanc, K.P. Koo, C.G. Askins, M.A. Putnam, E.J. Friebele, J. Lightwave Technol. 15 (1997) 1442.
[50] B.G. Potter Jr., M.B. Sinclair, J. Electroceram. 2 (1998) 295.